IEICE TRANS. COMMUN., VOL. E79–B, NO. 6 JUNE 1996

PAPER *Special Issue on Weather Radar Technology*

Validation and Ground Truth for TRMM Precipitation Radar Using the MU Radar

Toru SATO[†], **Toshihiro Teraoka**[†*], *and* **Iwane Kimura**[†], *Members*

SUMMARY The MU radar of Japan is one of important candidates for providing accurate ground truth for the TRMM precipitation radar. It can provide the dropsize distribution data together with the background atmospheric wind data with high accuracy and high spatial resolution. Special observation scheme developed for TRMM validation using the MU radar is described, and preliminary results from its test experiment are shown. The high-resolution MU radar data are also used in numerical simulations to validate the rain retrieval algorithm for the TRMM PR data analysis. Among known sources of errors in the rain retrieval, the vertical variability of the dropsize distribution and the partial beam-filling effect are examined in terms of their significance with numerical simulations based on the MU radar data. It is shown that these factors may seriously affect the accuracy of the TRMM rain retrieval, and that it is necessary to establish statistical means for compensation. However, suggested means to improve the conventional α-adjustment method require careful treatment so that they do not introduce new sources of errors.

key words: TRMM precipitation radar, MU radar, ground truth, rain retrieval algorithm, numerical simulation

1. Introduction

The largest advantage of space-borne measurements is in its global coverage, especially in the tropical area, where most of the rainfall occurs. TRMM (Tropical Rainfall Measuring Mission) satellite[1] will be the first one which installs a precipitation radar (hereafter referred to as PR)[2] onboard, and will be launched in 1997. It is expected to provide essential information in understanding the global water circulation. However, since the planned radar is a single-frequency, single-polarization, and non-Doppler one, the retrieval of rain intensity from the echo intensity data requires careful interpretation based on sophisticated algorithms which incorpolate with peripheral ground validation data.

The objective of this study is to 1) establish a reliable ground truth scheme for the planned TRMM PR using a ground-based radar, and 2) to validate the rain retrieval algorithm based on the radar data. While most of ground validation sites for TRMM PR use microwave Doppler weather radars, we use the the MU (Middle and Upper atmosphere) radar of Kyoto University, Japan. The MU radar, which is a large VHF Doppler radar designed to observe the earth's upper atmosphere, has a unique capability of measuring the vertical profile of the rain drop-size distribution (DSD) simultaneously with background atmospheric parameters such as winds and turbulence[3].

The vertical wind velocity and the intensity of turbulence provide a reliable measure of discriminating the convective and stratiform rains. Also, the radar is equipped with an active phased array antenna whose beam steerability roughly covers the footprint of TRMM PR with a much higher horizontal resolution. It is thus possible not only to provide an accurate radar reflectivity factor Z versus height, but also to quantitatively evaluate the partial beam filling error of TRMM PR. In total, the MU radar can provide a very accurate ground truth for TRMM PR, although limited to the cases in which the satellite passes over the radar site.

In this paper, We first examine the special observation scheme of the MU radar developed for TRMM PR ground truth experiments, and then study the effect of spatial valiability of the rain on the planned rain retrieval algorithm using numerical simulations based on the MU radar data.

2. Ground Truth Using the MU Radar

The MU radar is designed to have a sufficient sensitivity to detect backscattering from atmospheric turbulence, which is also called clear-air echoes, so that the background wind field and the strength of turbulence can be monitored continuously in time and height[4]. At the frequency of the MU radar, which is 46.5 MHz, the Rayleigh scattering from raindrops are received with similar intensity as the turbulence echo under precipitating conditions. It is thus possible to estimate accurate DSD compensated for the background atmospheric motion.

Another advantage of the MU radar for precipitation study is its beam steerability. The antenna beam direction can be changed arbitrarily from pulse to pulse within the visible range of 30° from the zenith. Recent upgrading of the data taking system of the MU radar enabled to obtain and process Doppler spectra from a much larger number of directions simultaneously than before[5].

Taking advantage of this improvement, we have developed a special observation scheme for TRMM PR ground validation. Basic system parameters of the MU radar for TRMM validation mode is given in Table 1. Figure 1 shows the arrangement of the radar beams. Large circle shows the footprint of TRMM PR, and small circles are the MU radar beams at 3-km height. These 19 beam directions are switched electronically at the pulse interval of 400μsec in a cyclic manner. Doppler echo power spectra are computed at a height interval of 150m for each beam direction

Manuscript received December 1, 1995.
Manuscript revised February 16, 1996.

[†]The authors are with the Department of Electronics and Communication, Kyoto University, Kyoto, 606-01, Japan.
[*]Presently, the author is with Matsushita Electric Industrial Co., Ltd.

Table 1 Basic parameters of the MU radar for the TRMM validation mode.

Parameter	Value
Location	Shigaraki, Shiga, Japan (34.85° N, 136.10° E)
Radar system	monostatic pulse radar; active phased array system
Operational frequency	46.5 MHz
Antenna	circular array of 475 crossed Yagi's
aperture	8330 m^2 (103 m in diameter)
beam width	3.6° (one way; half power for full array)
steerability	steering is completed in each IPP
beam directions	19; 0°–30° off zenith angle
polarizations	linear
Transmitter	475 solid state amplifiers (TR modules; each with output power of 2.4 kW peak)
peak power	1 MW (maximum)
average power	2.5 kW (duty ratio 0.25%)
bandwidth	1.65 MHz (pulse width: 1 μs)
IPP	400 μs
Receiver	
bandwidth	1.65 MHz
IF	5 MHz
A/D converter	12 bits × 8 channels
Pulse compression	none

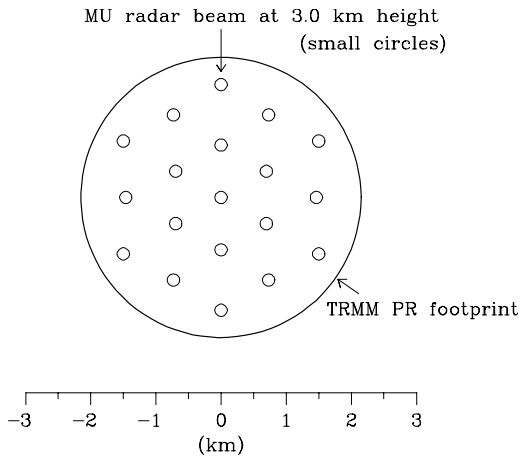

Fig. 1 Beam arrangement of TRMM PR and the MU radar at 3 km height.

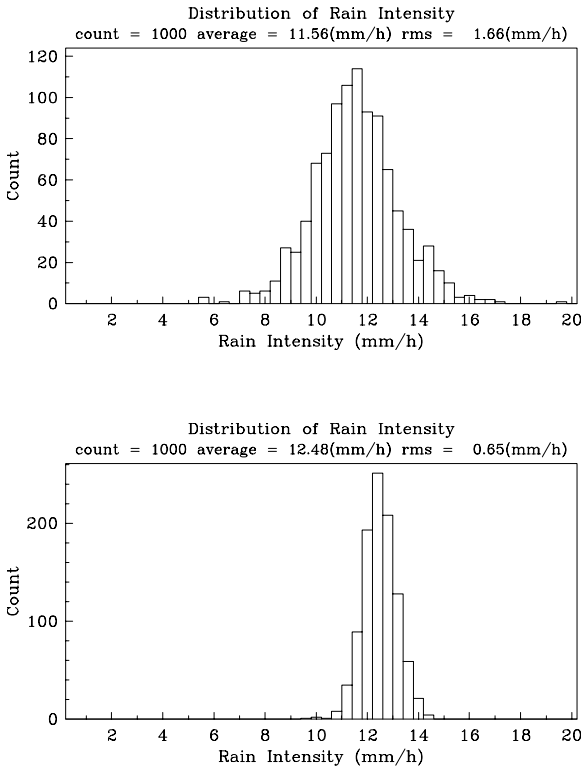

Fig. 2 Distribution of estimated rain intensity in numerical simulation. The given rain intensity is 12.6 mm/h. The top and bottom panels are for N = 5 and N = 30, respectively.

every 10 seconds, and averaged for 1 minutes. Rain drop-size distribution is estimated from the observed spectra by fitting the theoretical spectra assuming the gamma distribution[6]. Background wind and spectral broadening due to atmospheric turbulence are automatically compensated for by simultaneously fitting the atmospheric component[3].

The accuracy of derived rain and atmospheric parameters with the MU radar has been quantitatively evaluated by numerical simulations, and that of the rain intensity and wind velocity has been confirmed by observations. Figure 2 shows the result of estimated rain intensity by numerical simulations. Theoretical Doppler spectrum with typical precipitation and atmospheric condition is generated and distorted by statistical fluctuations whose magnitude is the same as that of the actual observation condition, averaged incoherently for N times, and then analysed by the fitting procedure. The figure shows the distribution of rain intensity estimated from 1000 spectra with the same theoretical spectrum but with different random numbers. The upper figure shows the distribution for N = 5, which corresponds to the time and height resolutions of 1 min and 150 m, respectively. The true rain intensity given in the simulation is 12.6 mm/h. The standard deviation of the estimated rain intensity is 1.66 mm/h. The error due to statistical fluctuations in the spectra is roughly constant for different rain intensity. The lower figure is the same as the upper one, but for N = 30, which corresponds to the time and height resolutions of 1 min and 900 m, re-

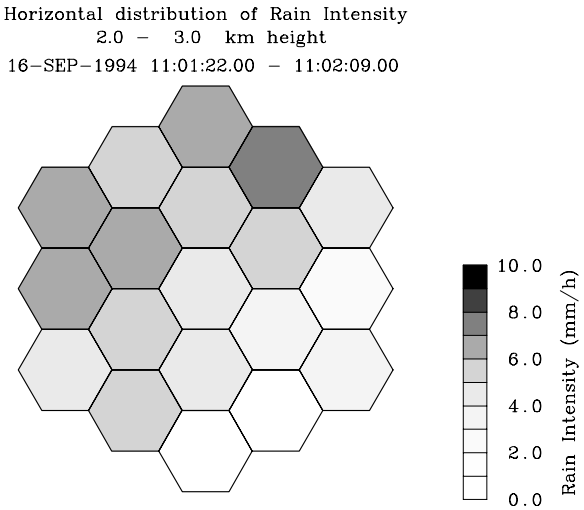

Fig. 3 An example of the horizontal distribution of rain intensity.

spectively. The standard deviation in this case is 0.65 mm/h, which is the expected accuracy of the MU radar rain estimate for a column average over 900 m in height.

Comparison of the accuracy with a ground-based rain gauge is a more difficult task due to the different sampling volume for the two sensors. We carefully chose steady stratiform rain situations so that spatial homogeneity is ensured, and compared the 1-min average rain intensity observed by the MU radar with a drop-counter type rain gauge, whose sensitivity is 0.002mm (0.12mm/h for 1-min resolution). The MU radar data were averaged for 900 m in height. It was found that the standard deviation between the two sensors is about 1 mm/h, confirming the theoretical expectation.

Figure 3 is an example of the horizontal distribution of the rain intensity observed during a convective rain event on September 16, 1994 with the 19-beam method. Each shaded hexagon denotes the rain intensity averaged for 1 min in 2-3 km height range at each beam direction shown in Figure 1. A much larger horizontal variation than the accuracy limit seen in this figure demonstrates the natural variablity inside a local rain event. Accumuration of such data will be of crutial importance in evaluating the partial beam-filling (PBF) error of the TRMM PR radar algorithms.

3. Rain Profiling Using Space-borne Radar Data

The most essential part of the precipitation radar signal prcessing is the conversion from the measured reflectivity factor into the rain intensity. The candidate algorithm for the rain profiling (2A-25) will be an extension of the α-adjustment method[7–9]. Here we briefly summalize the algorithm of the basic α-adjustment method[10].

We assume an exponential DSD which is expressed by

$$N(D) = N_0 \exp(-\Lambda D) \ , \tag{1}$$

where D is the drop diameter, and $N(D)$ is number density distribution. Further assuming that the scattering is in the Rayleigh region, the attenuation coefficient at a given range r from the radar is expressed as[11]

$$k(r) = \alpha Z(r)^{\beta} \ , \tag{2}$$

where $Z(r)$ is the reflectivity factor, which is related to the rain intensity $R(r)$ by

$$Z(r) = aR(r)^{b} \ . \tag{3}$$

The measured reflectivity factor Z_{m} is given by

$$Z_{\mathrm{m}}(r) = Z(r)[1 - qS(r)]^{-1/\beta} \ , \tag{4}$$

where

$$q = 0.2\beta \ln 10 \tag{5}$$

$$S(r) = \int_0^r \alpha Z_{\mathrm{m}}(s)^{\beta} \mathrm{d}s \ . \tag{6}$$

If the given parameters α and β are correct, Eqs. 4-6 can be solved to give the classical Hitschfeld-Bordan solution[12] of $Z(r)$, and thus $R(r)$, which is known to be sensitive to errors in the parameters when the attenuation is large. If the path-integrated attenuation (PIA) is given, it is possible to adjust α so that it satisfies the relation

$$A_{\mathrm{s}} = [1 - qS(r_{\mathrm{s}})]^{1/\beta} \ , \tag{7}$$

where A_{s} is the measured PIA factor, and r_{s} is the range of the sea surface. The PIA factor can be estimated from the magnitude of the echo from the sea surface assuming that the reflectivity of the sea surface in the precipitation area is the same as that of neighboring precipitation-free region.

Other three parameters β, a, and b are assumed to be constant. In this paper we use the following values based on the Marshall-Palmer $Z - R$ relation and an empirical $k - R$ relation[13] interpolated to the TRMM PR frequency of 13.8 GHz as the initial set of parameters.

$$\begin{array}{ll} a = 200 & b = 1.6 \\ \alpha = 5.06 \times 10^{-4} & \beta = 0.75 \end{array} \tag{8}$$

4. Effect of DSD Variations in Height

Extensive studies have been made to compare accuracies of different rain retrieval algorithms using numerical simulations as well as observed data[14–16, 9]. However, the main emphasis of these studies is on the comparison of different techniques, and contributions from individual sources of errors are not yet clearly identified. Among various sources of errors, the nature of the spatial inhomogeneity of rain is little known mainly because of the difficulty in observations.

We plan to quantitatively examine the effect of the vertical and horizontal inhomogeneity of rain on the accuracy of TRMM PR standard algorithms with numerical simulations of similar approach as we verified the accuracy of the MU radar data.

In this section we examine the effect of the height variations of DSD using the MU radar data as realistic examples of the given 'truth' in the simulation.

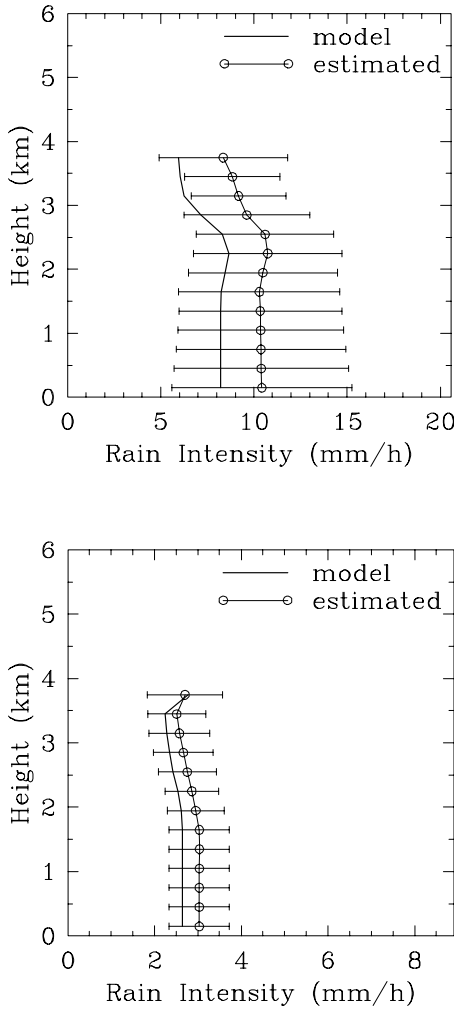

Fig. 4 Model and simulation results of rain profiling for the stratiform rain (left) and convective rain (right).

Since the α-adjustment method assumes that the parameters α and β are constant versus height, their height variation may cause errors in the derived rain intensity. Figure 4 shows the result of simulations using the real DSD profiles observed by the MU radar as model profiles. The upper figure is for stratiform rains, and the lower figure is for convective ones. The stratiform case consists of 135 profiles of 1-min resolution taken on July 2-4, 1990, when a stationary front associated with Baiu was present near the MU radar, and the convective case consists of 43 profiles taken on September 19, 1990, when a typhoon was passing near the MU radar. Determination of the rain type was made for individual 1-min profile by whether echoes from rain drops, which have larger Doppler shift than snowflakes, are observed above the freezing level or not. Only those profiles that satisfies this criteria for the stratiform rain for the former data set, and for the convective rain for the latter data set, respectively, are selected. All of these data are taken with the 5-beam method[5], which is routinely used for tropospheric observations with the MU radar. In this mode the beams are arranged within 10° from the zenith.

Rainfall parameters derived from the observed data for each beam at the same height are averaged, and two adjacent range gates of 150-m intervals are also averaged in order to simulate 250-m range resolution of TRMM PR. The k and Z factors at 13.8 GHz are computed for each range bin from the observed DSD, and then converted to $Z_{\rm m}$ profile. In order to avoid additional source of error associated with the bright band, we used the data only below the freezing level. Using these profiles as the given model values, we made numerical simulations. The α-adjustment method is applied to each 1-min profile and the rain intensity is estimated at each range bin. The result is averaged for the entire data set. The error bar put on each estimated value denoted by a circle indicates the standard deviation of the difference between the instantaneous model rain intensity and the estimated one. The error bar for the convective case is about twice larger than the stratiform case, probably due to larger vertical variations of DSD in the convective rain cells.

It should be noted that the vertical variation of DSD also causes positive bias errors even though the α adjustment correctly compensates for the path integrated attenuation. The bias at the sea surface level is 15% and 27% for the stratiform and convective cases, respectively. This bias error is due to the non-linearity in the $Z - R$ and $k - R$ relations. Although the bias is within the standard deviation, it has a significant meaning for TRMM project whose goal is to provide accurate rain intensity in one-month mean value. It will be effective to make statistical compensation for this vertical variability of DSD based on ground validation radar data.

5. Effect of Partial-Beam-Filling Errors

In the basic α-adjustment method, the rain is assumed to be uniform inside the PR radar beam. It is anticipated that the horizontal inhomogeneity of the rain causes systematic bias in the estimated attenuation, and thus in the rain intensity. In the standard algorithm 2A-25, it is planned to make use of variability of rain over adjacent beams to estimate the magnitude of inhomogeneity of the rain inside each beam[7].

A path-integrated parameter $\zeta_i = qS(r_{\rm s})$ is first computed for the beam of concern and for the neighboring $(M-1)$ beams. Here we use the adjusted α in Eq. 6. Then its standard deviation ξ defined by

$$\xi = \sqrt{\sum_{i=1}^{M}(\zeta_i - \zeta)^2/M} \tag{9}$$

$$\zeta = \frac{1}{M}\sum_{i=1}^{M}\zeta_i \tag{10}$$

is computed to express the magnitude of inhomogeneity inside each beam. It is assumed here that the small-scale inhomogeneity is equal to, or at least directly related to, the larger-scale inhomogeneity. Since these two parameters ζ and ξ represent the magnitude of the mean attenuation and

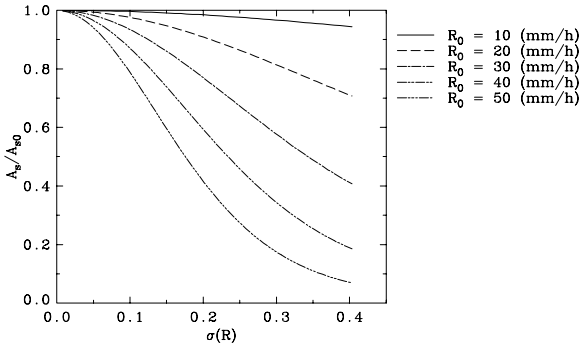

Fig. 5 The PIA correction factor A_s/A_{s0} versus the fractional standard deviation of rain intensity $\sigma(R)$.

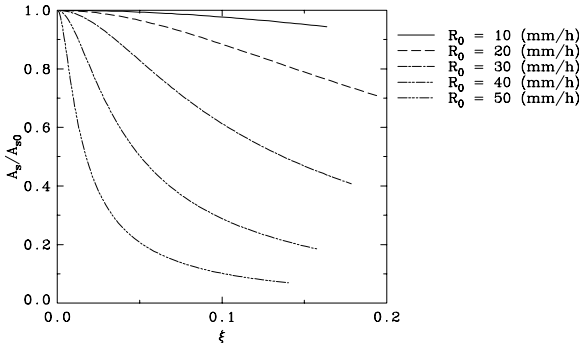

Fig. 6 The PIA correction factor A_s/A_{s0} as a function of measured inhomogeneity parameter ξ.

its horizontal variability, respectively, it is in principle possible to estimate the attenuation factor A_s compensated for the PBF effect. However, details of the compensation algorithm are not yet established, and require further study.

Here we briefly examine the nature of this compensation scheme by numerical simulations. We assume that the rain is uniform with height below 5 km, and randomly varies in the horizontal direction with no spatial correlation. It should be noted here that ξ is thus constant regardless to the footprint size of the radar beam. We fix N_0 to a constant value of 0.1 cm^{-4}, and change Λ so that the rain intensity R follows a Gaussian distribution with negative part truncated. The mean of the distribution of R after the truncation is denoted as R_0, and $\sigma(R)$ is used to denote the fractional standard deviation relative to R_0. The maximum value of $\sigma(R)$ is thus limited to about 0.4 due to the truncation. Since N_0 is constant, we can compute k and Z from the $R-Z$ and $k-Z$ relations for N_0 = 0.1 cm^{-4}. The Z_m profile is then computed for each point from these k and Z values, then the α-adjustment method is applied.

The derived rain intensity R_e is underestimated because the PIA is underestimated (the PIA factor A_s is thus overestimated) due to the horizontal variation of R. For example, R_e is underestimated by 17% at the sea surface level for R_0 = 30 mm/h and $\sigma(R)$=0.2. The error increases as R and $\sigma(R)$ increase.

If we can estimate the inhomogeneity correctly, it is possible to compensate for the effect by modifying the observed A_s so that it represents the PIA value of a uniform rain with the same intensity. Figure 5 shows the variation of the PIA correction factor A_s/A_{s0} versus $\sigma(R)$ for various values of R_0, where A_s and A_{s0} denotes the PIA factor for a uniform rain of rain intensity R_0, and the PIA factor to be observed by the TRMM PR, respectively. For the case of Figure 3, the correction is not necessary because R_0 is small even though $\sigma(R)$ is as large as 0.24. Accumulation of further data with the 19-beam method is important for obtaining quantitative information on the small-scale variability of the rain events.

In the real data analysis, the horizontal inhomogeneity of the rain is estimated via the parameter ξ. Figure 6 is the same as Figure 5 except that the abscissa is expressed in terms of ξ. Note that ξ takes a value of 0–0.2, since it is the standard deviation of ζ, which takes a value of 0–1. This figure clearly shows the large dependency of ξ on the mean rainfall rate R_0 even for very small ξ. For $R_0 > 10$ mm/h, for which the correction is important, it is essential to know not only the inhomogeneity factor ξ, but also the mean intensity of the rain.

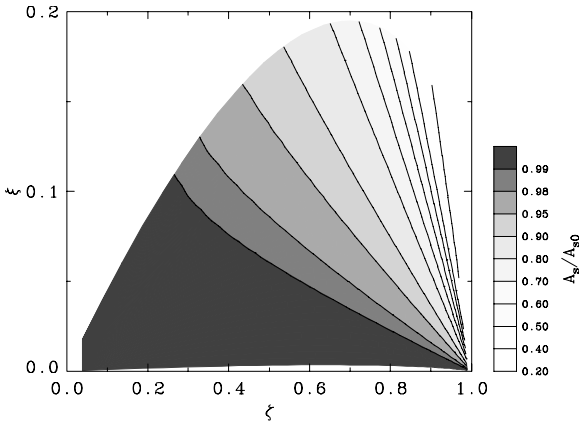

Fig. 7 PIA correction factor A_s/A_{s0} as a function of the two measurable parameters ζ and ξ.

Since R_0, which is the final parameter to be estimated, is not available in the estimation, we have to estimate the rain intensity through the parameter ζ. Figure 7 shows the PIA correction factor as a function of two measurable parameters ζ and ξ. It is thus possible to compensate for the PBF effect using this diagram if the inhomogeneity of rain inside the beam is the same as that derived from adjacent beams as assumed in the current simulation, or if it can be estimated from the larger scale inhomogeneity assuming some universal spectrum of the horizontal variability of the rain. Intensive studies using ground-based radars located in tropical regions is required in order to establish such spectrum.

Although the above procedure provides the correction factor, we have to be careful on its accuracy. Figure 7 clearly indicates that the correction factor is close to unity for most of the values of ζ and ξ, and decreases rapidly in a rather

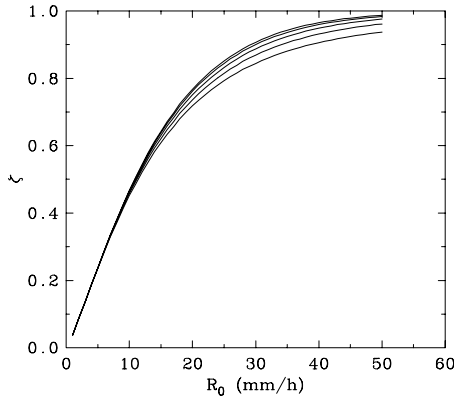

Fig. 8 Variation of ζ versus mean rain intensity R_0. Five curves are for $\sigma(R)$ values of 0–0.4.

narrow range of the parameters. Also, the attenuation factor ζ is not a linear function of R_0 as shown in Figure 8. Five curves in this figures are for different values of $\sigma(R)$ in its entire range of 0–0.4. For strong rains of more than 20 mm/h, attenuation becomes very large and ζ starts to saturate. In this region, 10% of error in ζ corresponds to an error of 10–20 mm/h in R. As Figure 7 shows, it is this range that the correction becomes essential. However, in actual observations ζ should be determined by the surface reference technique using the echo intensity from the ocean surface. Although its accuracy is not yet evaluated in detail, it will not be easy to maintain the absolute accuracy of 10%. It will be important to set some reliability criteria on the accuracy of the surface echo, probably using its variability in the area surrounding the current precipitation area.

6. Summary

An accurate mean of the ground truth for the TRMM precipitation radar has been developed with the MU radar. Preliminary experiment under a convective rain event showed a strong spatial inhomogeneity of the rainfall intensity. It has been confirmed that the MU radar will serve as an effective mean of ground truth for TRMM PR.

The MU radar data are also used in numerical simulations to evaluate the standard rain retrieval algorithm for the TRMM PR data analysis. Effect of the vertical variability of DSD was quantitatively examined, and it was found that it causes a bias of as large as 27% under convective conditions. The proposed scheme for compensating for the PBF error was also examined with a numerical simulation. It was pointed out that although it is possible to make the compensation, its accuracy highly depends on the accuracy of the sea-surface echo.

It is planned to apply some weighting function on the correction factor so that the error in various factors be minimized[7]. In order to establish the optimum weighting, it is needed to accumulate further quantitative study using ground validation experiments, especially using those in the tropical region.

Acknowledgment

The authors gratefully acknowledge Drs. T. Iguchi and T. Kozu of Communications Research Laboratory for their helpful comments and suggestions. This work was supported in part by Grant-in-Aid for Scientific Research (C) 06640559 of the Ministry of Education, Science and Culture, Japan. The MU radar belongs to, and is operated by Radio Atmospheric Science Center, Kyoto University.

References

[1] J. Simpson, R. F. Adler, and G. North, "A proposed Tropical Rainfall Measuring Mission (TRMM) satellite", *Bull. Amer. Meteor Soc.*, **69**, 278–295, 1988.

[2] K. Nakamura, K. Okamoto, T. Ihara, J. Awaka, and T. Kozu, "Conceptual design of rain radar for the tropical rainfall measuring mission", *Int. Satellite Comm.*, **8**, 257-268, 1990.

[3] T. Sato, H. Doji, H. Iwai, I. Kimura, S. Fukao, M. Yamamoto, T. Tsuda and S. Kato, "Computer processing for deriving drop-size distribution and vertical air velocities from VHF Doppler radar spectra", *Radio Sci.*, **25**, 961–973, 1990.

[4] T. Sato, T. Tsuda, S. Kato, S. Morimoto, S. Fukao and I. Kimura, "High-resolution MST observations of turbulence by using the MU radar", *Radio Sci.*, **20**, 1452–1460, 1985.

[5] S. Fukao, T. Sato, T, Tsuda, M. Yamamoto, M. D. Yamanaka and S. Kato, "MU radar: New capabilities and system calibrations", *Radio Sci.*, **25**, 477–485, 1990.

[6] T. Sato, M. Sato, H. Chotoku, I. Kimura, H. Ishida, and T. Harimaya, "Evolution of raindrop size distribution observed by a VHF Doppler radar", *Proc. Int. Symp. Antennas Propagat. 1992*, 1049–1052, 1992.

[7] T. Iguchi, "Status report of 2A-25 and issues", *Proc. TRMM Joint Radar Group Meeting*, 349–358, 1994.

[8] T. Iguchi, "Development of algorithms for retrieving three-dimensional rain profiles from TRMM precipitation radar and radiometer", *Proc. First TRMM Workshop*, 171–174, 1994.

[9] T. Iguchi and R. Meneghini, "Intercomparison of single-frequency methods for retrieving a vertical rain profile from airborne or spaceborne radar data", *J. Atmos. Ocean. Tech.*, **11**, 1507-1515, 1994.

[10] R. Meneghini, J. Eckerman, and D. Atlas, "Determination of rain rate from a spaceborne radar using measurements of total attenuation", *IEEE Trans. Geosci. Remote Sens.*, **GE-21**, 34–43, 1983.

[11] C. W. Ulbrich, "Natural variations in the analytical form of the raindrop size distribution", *J. Climate Appl. Meteor.*, **22**, 1764–1775, 1983.

[12] W. Hitshfeld and J. Bordan, "Errors inherent in the radar measurement of rainfall at attenuating wavelengths", *J. Meteor.*, **11**, 58–67, 1954.

[13] R. L. Olsen, D. V. Rogers, and D. B. Hodge, "The aR^b relation in the calculation of rain attenuation", *IEEE Trans. Antennas Propagat.*, **AP-26**, 318–329, 1978.

[14] R. Meneghini, K. Nakamura, C.W. Ulbrich, and D. Atlas, "Experimental tests of methods for the measurement of rainfall rate using an airborne dual-wavelength radar", *J. Atmos. Ocean. Tech.*, **6**, 637–651, 1989.

[15] J. Testud, P. Amayenc, and M. Marzoug, "Rainfall-rate retrieval from a spaceborne radar: Comparison between single-frequency, dual-frequency, and dual-beam techniques", *J. Atmos. Ocean. Tech.*, **9**, 599–623, 1992.

[16] M. Marzoung and P. Amayenc, "Improved range-profiling algorithm of rainfall rate from a spaceborne radar with path-integrated attenuation constant", *IEEE Trans. Geosci. Remote Sens.*, **GE-29**, 584–592, 1991.

Toru Sato was born on March 27, 1954. He received the B.E., M.E., and Ph.D. degrees in electrical engineering from Kyoto University, Kyoto, Japan in 1976, 1978, and 1982, respectively. He was a graduate student research associate of Arecibo Observatory, National Astronomy and Ionosphere Center from 1979 to 1980. He joined Radio Atmospheric Science Center of Kyoto University in 1983 as a research associate. He is now an associate professor at Department of Electronics and Communication, Kyoto University. His major research interests have been system design and signal processing for atmospheric radars, radar remote sensing of the atmosphere, observations of precipitation using radar and satellite signals, radar observation of space debris, signal processing for subsurface radars, and digital satellite communication. He was awarded Tanakadate Prize from the Society of Geomagnetism and Earth, Planetary and Space Sciences in 1986. He is a member of the Institute of Electronics, Information, and Communication Engineers of Japan, the Society of Geomagnetism and Earth, Planetary and Space Sciences, the Japan Society for Aeronautical and Space Sciences, the Institute of Electrical and Electronics Engineers, and American Meteorological Society.

Toshihiro Teraoka was born on March 7, 1970. He received the B.E. and M.E. in electrical engineering from Kyoto University, Kyoto, Japan in 1993 and 1995, respectively. His study topic in the graduate school was the observation of precipitation using the MU radar, and the evaluation of TRMM PR algorithms. He joined Matsushita Electric Industrial Co., Ltd. in 1995, where he is currently engaged in study and development of antennas and microwave circuits at Device Engineering Development Center.

Iwane Kimura was born on December 25, 1932. He received the B.E., M.E., and Ph.D. degrees in electrical engineering from Kyoto University, Kyoto, Japan in 1955, 1957, and 1961 respectively. Since 1960, he has been a staff of Kyoto University; Department of Electronics and Department of Electrical Engineering II where he is now a Professor radio engineering since 1971. He has also been a visiting Professor of Institute of Space and Astronautical Science from 1981 to 1991. From 1964 to 1965, he was a research associate at Radioscience Laboratory, Stanford University on leave from Kyoto University. His research interests have been in radio science; particularly remote-sensing of upper atmospheres by radar techniques, and space plasma physics, such as theoretical study on propagation and generation of radio waves in magnetospheric and ionospheric plasmas, plasma measurements by rocket-Doppler technique, and active wave experiments in space plasmas using scientific satellites. He was awarded Inada Memorial Prize in 1958, and Tanakadate Prize in 1961. He is a member of the Institute of Electronics, Information, and Communication Engineers of Japan, the Institute of Electrical Engineers of Japan, the Society of Geomagnetism and Earth, Planetary and Space Sciences, and the American Geophysical Union.